A Laser-Induced Graphene Bending Sensor Array for Localized Wrinkle Monitoring during Flax Fiber Fabric Forming

M. Amindehghan[1], R. Seethaler[1*], and A. S. Milani[1*]

[1] Composites Research Network-Okanagan Laboratory, School of Engineering, The University of British Columbia, Canada

* *Corresponding authors (rudolf.seethaler@ubc.ca, abbas.milani@ubc.ca)*

Keywords: *Flexible sensors; Textile composites; Laser-induced graphene; Wrinkles detection*

1. Abstract

Forming-induced wrinkles remain a critical challenge in the manufacturing of textile-reinforced composite parts, as they can compromise structural integrity and mechanical performance of the final part. Current methods for wrinkle detection largely depend on visual inspection or optical measurement systems, which may be limited in capturing real-time or sub-surface deformations. This study introduces a flexible sensor-based approach utilizing laser-induced graphene (LIG) on polyimide (PI) tape to create a customizable bending sensor array, capable of detecting and localizing out-of-plane deformations during composites forming. The developed continuous sensor array is particularly useful for long-fiber fabrics formability monitoring. It operates on the piezoresistive principle where resistance changes are correlated with local curvature caused by wrinkling. To assess the efficacy of the array, wrinkle formation was first induced and evaluated under the picture frame test, using a flax dry woven fabric reinforcement. The bending sensor array successfully captured the localized resistance increases corresponding to local wrinkle formation prior to full shear locking, and a strong correlation was observed between the signal amplitude and the wrinkles curvature. Subsequently, the flexible sensing system was implemented in a 3D vacuum forming setup to further assess its applicability in action. The results suggested that the LIG-based flexible sensor arrays can provide a low-cost, highly customizable alternative to conventional vision-based measurement systems.

2. Introduction

Today, textile-reinforced composites are widely used in lightweight structural applications due to their high specific strength and design flexibility. However, during forming processes such as draping, stamping, and vacuum forming, the fabric reinforcements can concurrently undergo deformation modes including shear, tension, and bending [1]. Among the potential forming defects, wrinkling is particularly critical, as it introduces out-of-plane distortions that can significantly reduce mechanical performance and structural integrity of the final part [2]. To understand and control such defect, several experimental techniques have been developed to monitor fabrics deformation during forming. Optical methods, such as Digital Image Correlation (DIC) [3], grid-based strain analysis [4], and photogrammetry [5] have been extensively used to capture full-field deformation and strain evolution. While these approaches provide valuable insights into in-plane deformation mechanisms, they are generally limited to surface measurements, require direct optical access, and are often difficult to implement in real-time industrial forming processes in 3D.

In recent years, flexible and wearable sensing technologies have emerged as promising alternatives for structural monitoring. Piezoresistive sensors based on conductive materials, including carbon nanotubes and graphene, have demonstrated high sensitivity to mechanical deformation and have been explored for strain and pressure sensing applications [6]. Studies have investigated the integration of such sensors into textile structures for in-situ monitoring [7]. However, the existing approaches primarily focus on in-plane strain sensing, with limited capability for detecting localized bending or curvature associated with wrinkle formation [8], [9].

Laser-induced graphene (LIG) has recently gained attention as a low-cost and scalable material for flexible sensor fabrication. LIG can be directly patterned on polyimide substrates using laser processing, enabling rapid prototyping of customizable sensing architectures [10]. Although LIG-based sensors have been successfully applied in strain and pressure sensing in other areas [11], their application for detecting out-of-plane deformation and wrinkle formation in textile composites remains largely unexplored.

In this work, a flexible LIG-based bending sensor array is designed to enable localized detection of wrinkles in woven fabric reinforcements. The sensor operates based on the piezoresistive response to curvature-induced strain and is designed to be aligned with fabric yarns pattern, and to selectively respond to out-of-plane deformation while remaining insensitive to in-plane shear. The performance of the proposed sensor system is evaluated through controlled bending characterization, picture frame testing, and 3D vacuum forming experiments, as follows.

3. Methodology and Fabrication

3.1. Bending Sensor Design and Principle

The proposed LIG/PDMS sensor operates based on the principle of piezoresistivity, whereby the electrical resistance varies in response to mechanical deformation. When the sensor is attached along the yarn direction of a woven fabric reinforcement, it experiences bending deformation upon wrinkle formation. During outward bending, the sensing layer is located above the neutral axis of the substrate, resulting in tensile strain within the conductive LIG network and a corresponding increase in electrical resistance. Conversely, inward bending would induce compressive strain and reduce the resistance, although this mode is less dominant in typical wrinkle configurations during forming. In contrast, in-plane shear deformation primarily causes rotation of yarns without inducing significant strain in the sensor. As a result, the sensor remains largely insensitive to shear while exhibiting a strong response to out-of-plane deformation (i.e., a decoupled shear-bending sensing; Figure 1).

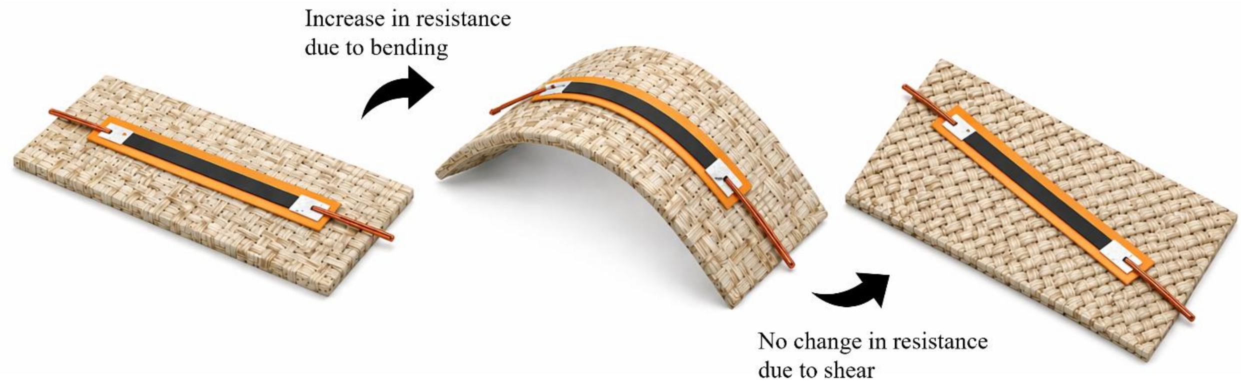

Figure 1 Schematic of the sensor working principle and how it changes resistance due to bending and shear deformation

3.2. Sensor Fabrication

The sensor fabrication process begins with defining the geometry and dimensions of the sensing element based on the target textile architecture. A UV laser is used to convert polyimide film (Kapton®, DuPont) into laser-induced graphene (LIG) through localized photothermal ablation (Figure 2a). The optimized laser processing parameters used in this study are summarized in Table 1. Electrical connections are established by attaching thin copper wires (AWG 34) to the LIG surface using conductive silver paste (MG Chemicals), followed by curing to ensure stable and low-resistance contact (Figure 2b). Finally, the sensor is encapsulated using polydimethylsiloxane (PDMS, Sylgard 184) with a base-to-curing agent ratio of 10:1, and cured at 100 °C for half an hour to provide mechanical protection and structural integrity (Figure 2c). Sensors were attached on a dry flax woven fabric (Lingrove Inc.) with 2×2 twill weave and density of 367-gsm.

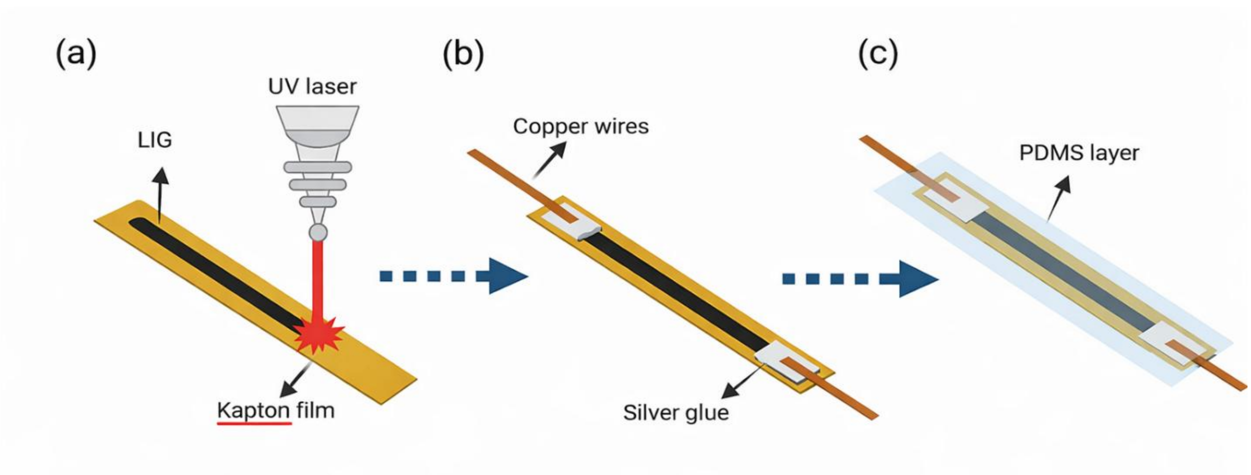

Figure 2. Bending sensor fabrication. (a) laser ablation; (b) electrode attachment; (c) PDMS encapsulation.

Table 1. Laser setting for LIG fabrication.

Power (mW)	**Defocus level (mm)**	**Frequency (kHz)**	**Speed (mm/s)**
500	4	40	10

4. Sensor Characterization

Before deployment in forming-induced wrinkle applications, the bending response of the sensor must be characterized directly. The three-point bending test based on ASTM D790 was adopted for this purpose. Although this standard is primarily intended for rigid polymer specimens, it provides a controlled method to induce out-of-plane deformation that is comparable to wrinkle formation in textile reinforcements. A specimen of dry flax fabric was prepared, and the sensor was attached along its surface. The support span was set to 2.5 in. Five sensors were tested under identical conditions, and the average response along with the standard error is presented in Figure 3(a). The radius of curvature was approximated by assuming a circular arc geometry of the specimen. The curvature radius R was calculated based on the chord length L and the mid-span deflection (sagitta) δ, as expressed in Eq. (1) [12]. This approximation enables correlation between the applied deformation and the measured resistance change of the sensor.

$$R = \frac{L^2}{8\delta} + \frac{\delta}{2} \tag{1}$$

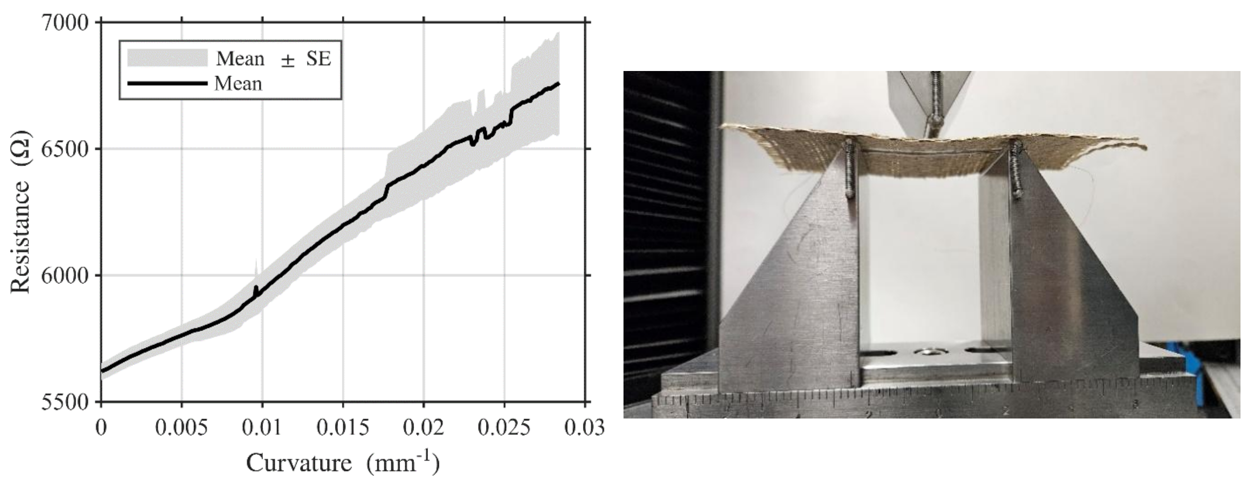

Figure 3 Three-point bending test and the resistance reponse of the sensor

5. Results and Discussion

5.1. Picture frame test

Wrinkle formation in woven fabrics is primarily driven by excessive in-plane shear deformation. To investigate this behavior, the picture frame test (PFT) was employed [13]. Two sensors were mounted on a flax fabric specimen, one at the center and the other along the arm of the sample, and the test was performed using a picture frame fixture (Figure 4). The response of the sensors during the test is presented as a function of shear angle. Both sensors exhibit negligible resistance change during the initial stages of deformation. However, at approximately ~20° sensor 1 started to show decrease in resistance which turned back to increase at ~33° global shear angle. On the other hand, sensor 2, show a noticeable increase in resistance starting at ~30°. While both sensors demonstrated the onset of the localized out-of-plane deformation, sensor 1 experience compression before the onset of wrinkle which manifested in slight resistance reduction. This closely aligns with the earlier studies where it was reported that the yarn local in-plane bending close to the jaws (due to clamping) can cause the shear rate at the center region to be faster than the frame (i.e., inducing a mismatch factor on shear deformation across the sample) [14]. Although the locking angle, estimated from the force response, occurs at approximately 55°, visual observations confirm that significant local wrinkle formation begins well before this point, consistent with findings reported in the literature [15]. This comes from the fact that the force response is representative of the entire sample, and cannot show the localized onset of defect in each region of interest. The sensor responses correlate well with the development of wrinkles, demonstrating the capability of the proposed system to detect early-stage wrinkle formation prior to complete shear locking.

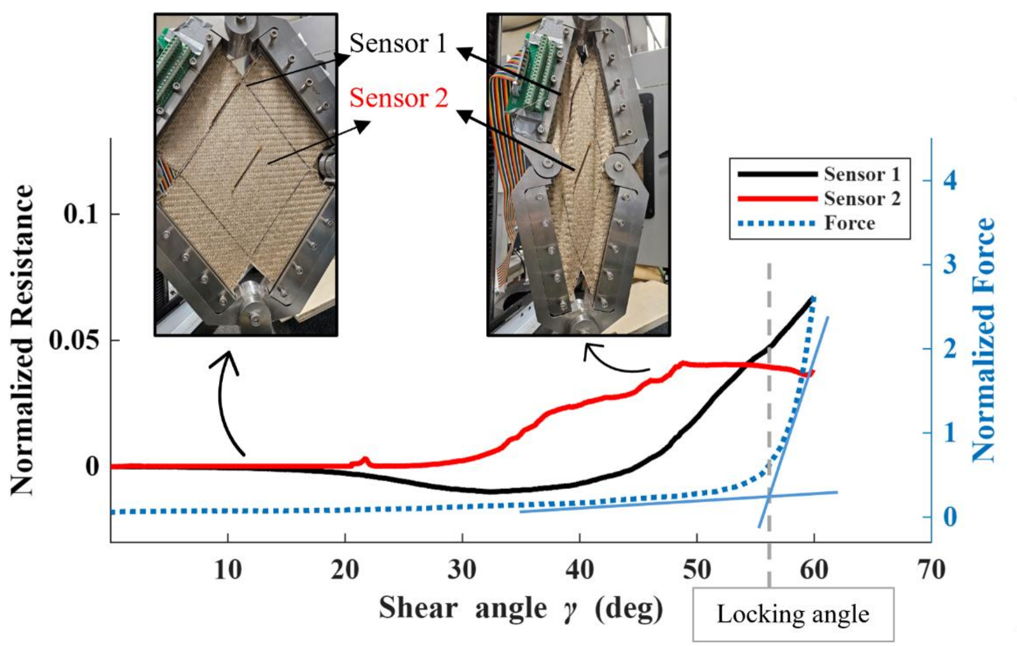

Figure 4 Response of the sensors in the picture frame test

5.2. 3D vacuum forming test

The next step was to evaluate the performance of the sensors under a realistic forming process. Various preforming techniques exist for textile reinforcements, including draping, stamping, and vacuum forming. In this study, a 3D vacuum forming process using a tetrahedral mold was selected. Two layers of flax fabrics were stacked with a 45° orientation relative to each other. Bending sensors were strategically placed in a way to enable detection of localized defects: two sensors were positioned on inclined surfaces of the mold, while a third sensor was placed on a flat region to serve as a reference (Figure 5). Two series of tests were conducted. In Test 1, no wrinkles were present in the formed fabric, whereas in Test 2, a wrinkle formed around Sensor 2 area. However, two key challenges arise in interpreting the sensor response in such 3D tests:

- Both mold geometry (upon contact with the fabric) and wrinkle formation can concurrently induce bending, leading to increased resistance and making it difficult to distinguish between the two causes.
- During vacuum bagging, the applied pressure introduces additional deformation in the sensor, contributing to resistance changes unrelated to forming defect.

The total measured resistance change can therefore be expressed as:

$$\Delta R_{sensor} = \Delta R_{mold} + \Delta R_{vacuum} + \Delta R_{defect} \quad (2)$$

To compensate for the mold geometry, a calibration step was introduced prior to forming. Each sensor on the fabric was manually pressed onto the mold surface to capture the local curvature-induced response, and the corresponding resistance change was recorded (Figure 6a). This provides an expected baseline response due solely to mold geometry.

To account for the vacuum pressure effect, the reference sensor—located on a flat region and remaining free of defects upon forming (Figure 5b)—captures the resistance change induced by pressure alone. By subtracting both the mold and reference sensor contributions, the defect-induced response can be isolated:

$$\Delta R_{sensor,adjusted} = \Delta R_{sensor} - \Delta R_{mold} - \Delta R_{Ref.sensor} = \Delta R_{defect} \quad (3)$$

$$DI = \frac{\Delta R_{defect}}{R_0} \quad (4)$$

All resistance changes were normalized with respect to their initial values to eliminate sensor-to-sensor variability ($R_n = \frac{\Delta R}{R_0}$). The resulting normalized adjusted resistance, defined as the Defect Index (DI) (Eq. 4), is presented in Figure 6(c) for both tests. In Test 1 (no wrinkle), Sensor 2 exhibits a DI close to zero, while Sensor 1 shows a negative value (~−0.1). In Test 2 (with wrinkle across Sensor 2), Sensor 2 shows a positive DI (~+0.1), indicating induced out-of-plane deformation due to wrinkle formation. In contrast, Sensor 1 maintains again a negative DI, which is attributed to local bridging where the fabric does not fully conform to the mold, resulting in reduced curvature compared to the nominal shape; i.e., leaving a gap/suspended region between the fabric and the tool surface.

These results demonstrate that the sensing system can effectively distinguish between different types of forming-induced defects. Specifically, wrinkles are associated with positive DI values, while bridging is characterized by negative DI values. A threshold can be defined to account for measurement uncertainty and enable reliable defect detection.

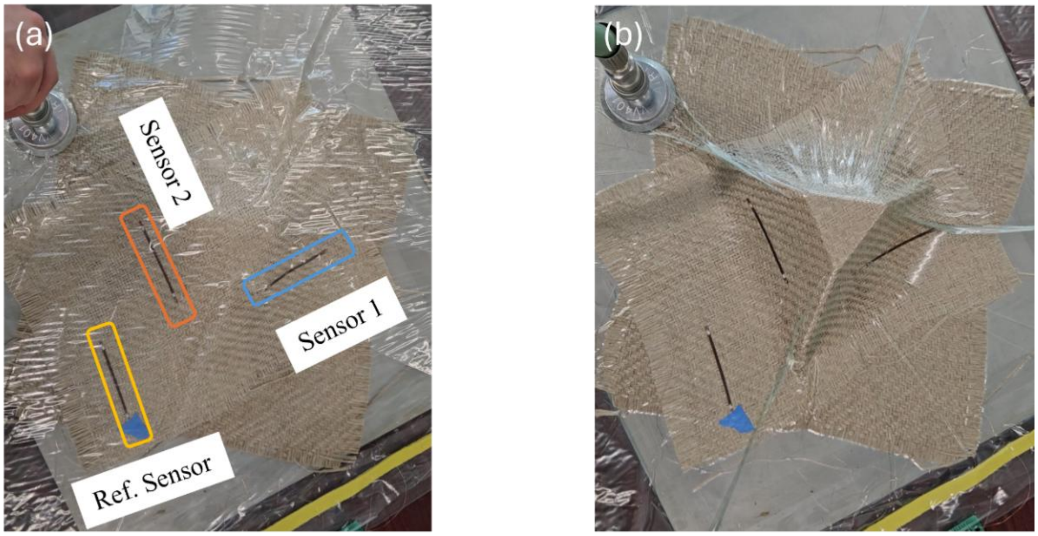

Figure 5 3D vacuum forming of two-plies of flax fiber on a tetrahedral mold. Sensors position (a) before and (b) after applying vacuum

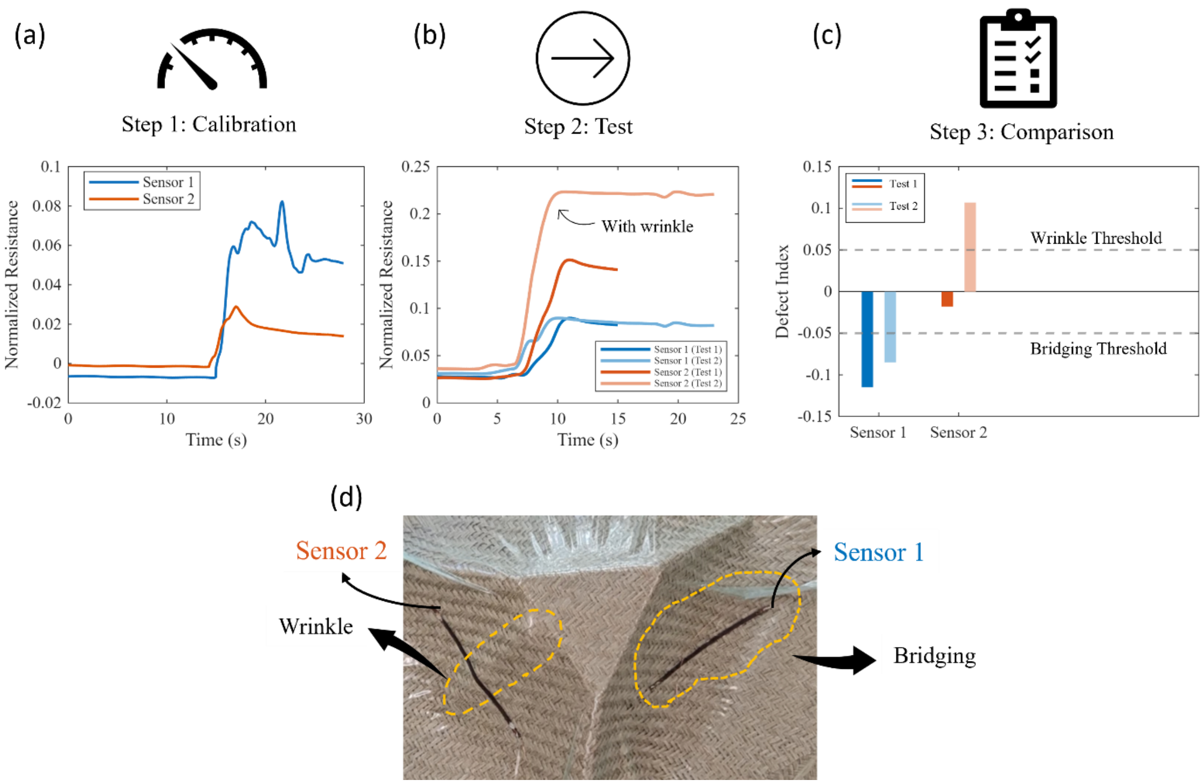

Figure 6 (a) Calibration of the bending sensors, (b) sensors' response in tests 1 and 2, (c) defect index for each sensor for tests 1 and 2, (d) sensor 1 and 2 on the wrinkle and bridging spots under test.

6. Conclusion and Future Steps

Flexible bending sensors based on LIG/PDMS were designed and demonstrated as an effective approach for monitoring out-of-plane defects, such as wrinkling and bridging, in textile reinforcements. The results confirm that the sensor response is directly correlated with local curvature, enabling reliable detection of bending-induced deformation. Due to their selective sensitivity to out-of-plane deformation and minimal response to in-plane shear, the sensors were able to detect wrinkle initiation at early stages, prior to the onset of eventual shear locking. Furthermore, the incorporation of a reference sensor in the 3D vacuum forming setup enabled separation of defect-induced signals from mold geometry and vacuum pressure effects. This led to the definition of a **Defect Index (DI)**, which allows differentiation between wrinkles (positive DI) and bridging (negative DI). Overall, the proposed sensing approach, albeit in early stage of its development, can provide a low-cost and highly customizable solution for real-time monitoring of forming quality in textile composites, with potential advantages over conventional optical measurement techniques. Future study should focus on:

- Extending the verification of the sensor to different textile reinforcements and forming processes.
- Embedding the sensors within mid-layers of composite preforms, where optical methods are not applicable.
- Developing closed-loop control strategies in which forming parameters are actively adjusted based on real-time sensor feedback
- Response of the sensor can be studied under effects from other defects modes (e.g., pre-forming misalignment inherent to the fabrics [16])

7. References

[1] U. Sachs *et al.*, "Characterization of the dynamic friction of woven fabrics: Experimental methods and benchmark results," *Compos. Part A Appl. Sci. Manuf.*, vol. 67, pp. 289–298, Dec. 2014, doi: 10.1016/J.COMPOSITESA.2014.08.026.

[2] Y. Zhang *et al.*, "A review of the formability of woven fabrics for composite materials," *Polym. Compos.*, vol. 45, no. 16, pp. 14498–14520, Nov. 2024, doi: https://doi.org/10.1002/pc.28837.

[3] R. S. Pierce, B. G. Falzon, M. C. Thompson, and R. Boman, "A Low-Cost Digital Image Correlation Technique for Characterising the Shear Deformation of Fabrics for Draping Studies," *Strain*, vol. 51, no. 3, pp. 180–189, Jun. 2015, doi: https://doi.org/10.1111/str.12131.

[4] B. Schäfer *et al.*, "Experimental analysis of the forming behavior of uni- and bidirectional non-crimp fabrics for different geometries," *Compos. B Eng.*, vol. 287, p. 111765, 2024, doi: https://doi.org/10.1016/j.compositesb.2024.111765.

[5] H. Krieger, A. Schnabel, L. Appel, and T. Gries, "Experimental Setup to Validate Textile Material Models for Drape Simulation," *Key Eng. Mater.*, vol. 554–557, pp. 456–464, 2013, doi: 10.4028/www.scientific.net/KEM.554-557.456.

[6] S. Yang, Y. Chen, and C. Jiang, "Strain engineering of two-dimensional materials: Methods, properties, and applications," Apr. 01, 2021, *Blackwell Publishing Ltd*. doi: 10.1002/inf2.12177.

[7] M. S. Irfan, T. Khan, T. Hussain, K. Liao, and R. Umer, “Carbon coated piezoresistive fiber sensors: From process monitoring to structural health monitoring of composites – A review,” *Compos. Part A Appl. Sci. Manuf.*, vol. 141, Feb. 2021, doi: 10.1016/j.compositesa.2020.106236.

[8] J. Fial, S. Carosella, L. Ring, and P. Middendorf, “Shear Characterization of Reinforcement Fabrics using Textile-applied printed Strain Sensors,” in *Procedia Manufacturing*, Elsevier B.V., 2020, pp. 65–70. doi: 10.1016/j.promfg.2020.04.134.

[9] C. Dufour, F. Boussu, P. Wang, and D. Soulat, “Local strain measurements of yarns inside of 3D warp interlock fabric during forming process,” *International Journal of Material Forming*, vol. 11, no. 6, pp. 775–788, 2018, doi: 10.1007/s12289-017-1385-0.

[10] J. Lin *et al.*, “Laser-induced porous graphene films from commercial polymers,” *Nat. Commun.*, vol. 5, no. 1, p. 5714, 2014, doi: 10.1038/ncomms6714.

[11] H. Wang, Z. Zhao, P. Liu, and X. Guo, “Laser-Induced Graphene Based Flexible Electronic Devices,” *Biosensors (Basel)*., vol. 12, no. 2, p. 55, Jan. 2022, doi: 10.3390/bios12020055.

[12] T. Pelli and T. P. Leonard, *Circles: Relationships with Segments and Angles*. in Studies in Geometry Series. Garlic Press, 2004. [Online]. Available: https://books.google.ca/books?id=DU1MAAAACAAJ

[13] M. Haghi Kashani, A. Hosseini, F. Sassani, F. K. Ko, and A. S. Milani, “The Role of Intra-Yarn Shear in Integrated Multi-Scale Deformation Analyses of Woven Fabrics: A Critical Review,” May 04, 2018, *Taylor and Francis Inc.* doi: 10.1080/10408436.2017.1342597.

[14] H. Montazerian, A. Rashidi, M. Hoorfar, and A. S. Milani, “A frameless picture frame test with embedded sensor: Mitigation of imperfections in shear characterization of woven fabrics,” *Compos. Struct.*, vol. 211, pp. 112–124, 2019, doi: https://doi.org/10.1016/j.compstruct.2018.11.096.

[15] M. H. Kashani, A. Rashidi, B. J. Crawford, and A. S. Milani, “Analysis of a two-way tension-shear coupling in woven fabrics under combined loading tests: Global to local transformation of non-orthogonal normalized forces and displacements,” *Compos. Part A Appl. Sci. Manuf.*, vol. 88, pp. 272–285, Sep. 2016, doi: 10.1016/j.compositesa.2016.06.004.

[16] A. S. Milani, J. A. Nemes, R. C. Abeyaratne, and G. A. Holzapfel, “A method for the approximation of non-uniform fiber misalignment in textile composites using picture frame test,” *Compos. Part A Appl. Sci. Manuf.*, vol. 38, no. 6, pp. 1493–1501, 2007, doi: https://doi.org/10.1016/j.compositesa.2007.01.008.